Aggregation and Gelation Effects on the Performance of Poly(3-hexylthiophene)/Fullerene Solar Cells

W. Y. Huang,*,† P. T. Huang,‡ Y. K. Han,§ C. C. Lee,† T. L. Hsieh,† and M. Y. Chang†

Department of Photonics and Semiconductor Technology Research and Development Center, National Sun Yat-Sen University, Kaohsiung, Taiwan, Department of Chemistry, Fu-Jen Catholic University, Taipei, Taiwan, and Department of Chemical Engineering, National Kaohsiung University of Applied Sciences, Kaohsiung, Taiwan

Received June 18, 2008; Revised Manuscript Received August 12, 2008

ABSTRACT: Poly(3-hexylthiophene) formed gels and showed liquid crystalline structures at high concentrations. The absorption properties of poly(3-hexylthiophene) showed dramatic changes during gelation, which is an indication of strong intermolecular π-electronic coupling of the ordered self-assembled poly(3-hexylthiophene) gels. The effect of conformational transitions on the photovoltaic properties of solution-processed poly(3-hexylthiophene)/fullerene blends has been studied in this Article. It is shown that the photovoltaic performance is strongly affected by gelation, which alters the morphology of the photoactive layer. Device optimization yields solar cells with a power conversion efficiency of 3.78% under standard test conditions (AM 1.5, 100 mW/cm^2).

Introduction

Converting solar energy into electrical energy is becoming ever more important due to the crisis in conventional energy sources. Organic solar cells (OSCs)[1−13] that are based on conjugated polymers have attracted much attention because of their potential advantages, including low cost of fabrication, ease of processing, mechanical flexibility, and versatility of chemical structure, as a result of the advances in organic chemistry. However, the low efficiency of these organic solar cells limits their feasibility for commercial use. The efficiencies of polymer photovoltaic (PV) cells got a major boost with the introduction of the bulk heterojunction concept.[7,8] Conceptually, the formation of bulk heterojunction phase allows for bulk separation of photoinduced excitons and high-mobility removal of electrons through the nanophase. Poly(3-hexylthiophene) (P3HT) has been the most used p-type material[9,10] in PVs, along with a fullerene derivative, [6,6]-phenyl C61-butyric acid methyl ester (PCBM), as an electron acceptor. However, the difficulty in these systems arises when we account for the effects of morphological modifications in P3HT phase due to the introduction of nanophase.[1,2,11] There are a significant number of studies that investigate the effects of processing parameters on blended photoactive nanophase. Berson and Xin et al.[11] have reported the effects of supramolecular assembly of regioregular poly(3-alkylthiophene)s into nanofibrils and nanowires, respectively, and the results make a great impact on the performance of photovoltaic cells. In addition, the molecular weight[12] and regioregularity[13] of P3HT also affect the performance of P3HT/PCBM devices.

In this work, dynamic gelation behavior was performed to elucidate the conformational transitions in the gel solutions of P3HT, and its effect on the efficiency of the PV devices was also studied. The intermolecular association and supramolecular organization in dilute solution of P3HT has been reported elsewhere,[14−17] and the morphological dependence of the performance of organic PV devices has also been reported.[5,11] However, the gelation behavior in concentrated solution and the effect of the conformational transitions during fabrication of the PV device on power conversion efficiency (PCE) have not been reported. Our experiment revealed that the performance of polymeric PV devices greatly depends on the fabrication conditions of the polymer thin film, primarily the aging time and its procedures. Therefore, we tried to systematically investigate the optimum aging conditions (temperature, time, and procedure) for the most efficient PV device.

Experimental Section

Materials. P3HT was prepared according to literature methods.[18] At the end of the polymerization procedure, the reaction mixture was poured into a large excess of methanol. The precipitate was collected and subjected to extraction in a Soxhlet extractor with methanol, followed by chloroform. The chloroform-soluble fraction of P3HT was used in this study. All of the other chemicals including PCBM and poly(methylmethacrylate) {PMMA} (M_w = 50 000) and solvents used in this study were purchased from Aldrich and used without further purification. Spectroscopic grade *o*-xylene was used for preparing polymer solutions. All polymer solutions were prepared by stirring solutions at 90 °C overnight.

Characterization. UV spectra were recorded using a DMS-300 spectrophotometer. The fluorescence spectra were collected by using a Perkin-Elmer LS-50B luminescence spectrophotometer, where the solid-state emission was performed in the 30°/60° angle geometry. A polarized optical microscope (POM, Nikon Optihot) was employed to observe liquid crystal and morphological textures of the polymer sols and gels. Gel permeation chromatography (GPC) analysis was conducted with a Polymer Laboratories HPLC system using polystyrene as the standard and tetrahydrofuran as the eluent. The result shows the number average molecular weight (M_n) of P3HT is 41 000, which corresponds to about 247 repeating units. The polydispersity index (M_w/M_n) is about 1.68.

Device Fabrication. Devices were fabricated on glass/ITO substrates. After the ITO was cleaned, a 15 nm thick poly(ethylenedioxy-thiophene)/poly(styrenesulfonic acid) (PEDOT/PSS, Baytron AI4083) was spin-coated. Subsequently, the photoactive layer (ca. 100 nm) consisting of P3HT blended with PCBM 1:1 by wt was spin-coated on the top of the PEDOT/PSS layer from a 1.0 wt % *o*-xylene solution. The metal electrode (Al, 200 nm) was thermally deposited through a shadow mask to make cells with an active area of 4 mm^2. $I-V$ curves were recorded with a Keithley 2400 source meter by illuminating the cells with 100 mW/cm^2 white light from a Steuernagel solar simulator to realize AM 1.5 conditions. For comparison, all cells were prepared without any optimizations, measured at ambient conditions, and were tentatively

* To whom correspondence should be addressed. Phone: 886-7-5252000ext. 4444. Fax: 886-7-5254499. E-mail: wyhuang@mail.nsysu.edu.tw.
† National Sun Yat-Sen University.
‡ Fu-Jen Catholic University.
§ National Kaohsiung University of Applied Sciences.

10.1021/ma801368z CCC: $40.75
Published on Web 09/30/2008

Table 1. Gel Formation Properties of P3HT in *o*-Xylene at Room Temperature

conc. (wt %)	gelation	gelation time [a]	turbidity
0.05	no		
0.1	NI [b]		
0.2	yes	4 weeks	clear
0.5	yes	2 weeks	clear
1.0	yes	24 h	clear
1.0	yes	1 weeks	turbid
2.0	yes	2 h	turbid
5.0	yes	0.5 h	turbid

[a] Measured by the inverted tube method. [b] It is too ambiguous to be identified.

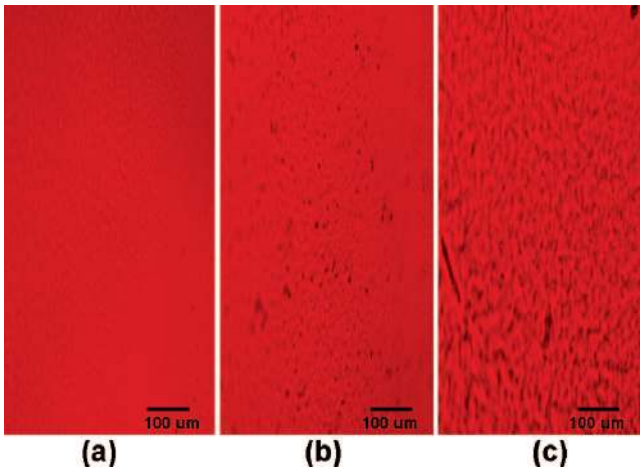

Figure 1. Crossed polarized photographs of the P3HT pristine thin films spin-coated from different solution concentrations: (a) 0.02 wt %, (b) 0.5 wt %, and (c) 1.0 wt %.

divided into two groups with and without filtration of the photoactive material solutions.

Results and Discussion

Gel Formation. To increase our understanding of the aggregation/gelation phenomenon of P3HT, we report here on a study of molecular aggregation in the sol and gel states of P3HT in *o*-xylene under air atmosphere. Gel formation was observed visually after the *o*-xylene solution was allowed to stand at room temperature for periods of up to several weeks. The visual observations are compiled in Table 1. It is worth emphasizing that (1) for the concentrated P3HT solutions gelation occurred at concentrations as low as 0.2 wt %, although the gelation time at room temperature could be weeks, whereas for the dilute solutions (<0.2 wt %) gelation was not observed; (2) P3HT formed transparent gels at low concentrations (<0.5 wt %) but turbid gels at high concentrations (>2 wt %), and both forms of gel were observed at concentrations in between, which depended on the time of aging. For the turbid gels, phase separation must have taken place during structural development. This indicates that the nature of the concentration, that is, the distance between molecules, has a dominant influence on gelation.

Polarized Optical Microscopy. Crossed polarized photographs of the spin-cast films of P3HT are shown in Figure 1. After standing at room temperature for 2 h, the film coated from the 1.0 wt % solution showed a clear morphological feature of aggregates (Figure 1c). However, when the concentration of solutions was decreased (0.5 wt %), a smaller number of aggregate domains was presented (Figure 1b), which were no longer seen in the film coated from the 0.02 wt % solution (Figure 1a). Certainly, nanostructured aggregates responsible for variation in photovoltaic properties could be observed using

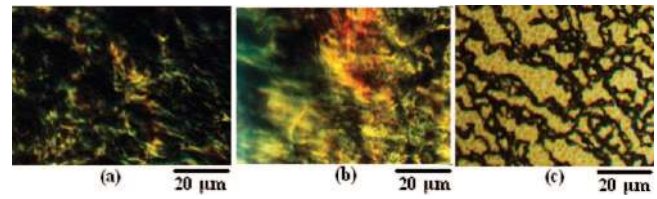

Figure 2. Polarized optical micrographs of P3HT in *o*-xylene at room temperature: (a) 28 wt % after 48 h and (b) 52 wt %, and (c) fibril structure prepared by flashing off the solvent.

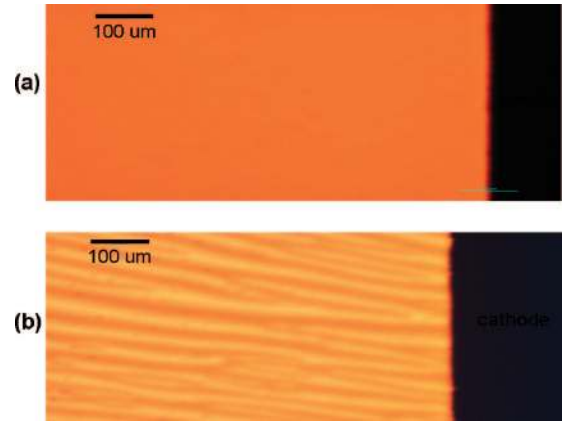

Figure 3. Crossed polarized photographs of the P3HT/PCBM devices fabricated from different photoactive material solutions: (a) without and (b) with filtration.

nanoscaled measurements, such as AFM (see Supporting Information). After standing at room temperature for several minutes to 4 weeks, depending on the concentrations, P3HT solutions turned into gels. The minimum concentration for gelation was about 0.2 wt %. However, birefringence was observed only when the polymer concentration was above a certain critical value, about 28 wt % in *o*-xylene. Optical micrographs revealed nematic liquid crystalline structures (Figure 2a) in only a few small domains, while the rest of the sample was isotropic (dark regions). Birefringence disappeared upon heating; in the meantime, the solvent was evaporated slowly to increase the concentration for the subsequent observation. After partial solvent evaporation, the sample was cooled to room temperature, and the concentration was determined by weighing. At the sample concentration of about 52 wt %, birefringent domains filled nearly the whole sample, and nematic texture (Figure 2b) was clearly identified. The same procedure was repeated to remove more solvent, but the texture remained almost unchanged, except for some growth in the size of the domain. On the other hand, fibril structures (Figure 2c) were observed when the sample was prepared by flashing off the solvent. In addition, upon the PCE measurement of devices (stated in later sections), it was apparent that the data could be categorized into two groups with different device fabrication process: with and without solution filtration, respectively. We then took photographs (Figure 3) for the two different groups of devices and found that a more orderly aligned morphology (Figure 3b) was observed in the device fabricated from filtered solutions, which was not seen in the device fabricated without filtered solutions (Figure 3a).

Photophysical Characterization. UV−Vis Absorption Spectra. Yamamoto and his co-workers[17] reported that the addition of methanol to P3HT solution in chloroform affords a colloidal solution. Such a transformation accompanied a concentration independent bathochromic shift of the $\pi-\pi^*$ absorption band from $\lambda_{max} = 450$ nm (in chloroform) to $\lambda_{max} = 520$ nm with

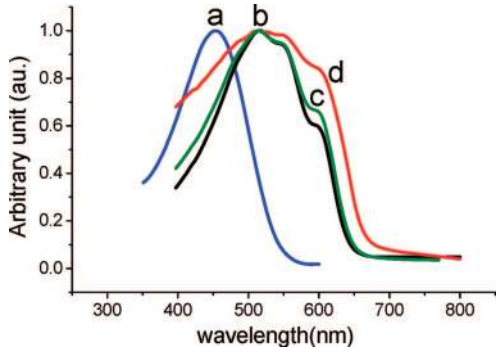

Figure 4. UV absorption spectra of the P3HT thin films cast from (a) dilute *o*-xylene solution (0.002 wt %) of the blend P3HT:polymethacrylate 1:10 by wt, (b) 1.0 wt % freshly prepared *o*-xylene solution of the P3HT, (c) 1.0 wt % aged *o*-xylene solution of the P3HT, and (d) 1.0 wt % aged *o*-xylene solution of the P3HT and then annealed at 150 °C for 10 min.

two shoulders at 560 and 610 nm in chloroform−methanol 1/1 (v/v) mixture. On the basis of the results reported by Yamamoto et al., and our previous morphological observations, we then utilized UV absorption analysis to realize the transit of molecular organization in thin films after quenching the system from the various solution states to solid thin films. The UV absorption spectra of P3HT (Figure 4) featured absorption bands at 455, 550, 600, and 640 nm, respectively, due to the different molecular organizations that result in various effective conjugation lengths, and hence different absorption band structures; this agrees well with the results published by Yamamoto et al. Upon the thin film (curve 4a) spin-coated from dilute *o*-xylene solution (0.002 wt %) of the blend P3HT:polymethacrylate 1:10 by wt, the absorption spectrum presented only an absorption of λ_{max} at 455 nm; however, the $\pi-\pi^*$ absorption band was shifted to $\lambda_{max} = 550$ nm with two shoulders at 600 and 640 nm, as the thin film (curve 4b) was solvent-cast from 1.0 wt % freshly prepared *o*-xylene solution of the P3HT, and the absorption band at 640 nm grew up when the thin film (curve 4c) was solvent-cast from 1.0 wt % aged *o*-xylene solution of the P3HT (gelatin like) and then annealed at 150 °C for 10 min. This could be ascribed to, in diluted liquid and/or solid solutions, the molecules acting as individuals or isolated chains[19,20] independent from each other, and thus the $\pi-\pi^*$ absorption band was blue-shifted when compared to those of the thin films solvent-cast from 1.0 wt % freshly prepared and aged *o*-xylene solutions, where eventually gels were formed and thus long-range order results in the prevalence of liquid crystalline domains or aggregates where the role of interpolymer interactions in electronic and photophysical properties becomes paramount. We therefore conclude that the $\pi-\pi^*$ absorption band and photophysical properties of P3HT thin films are really tunable by carefully manipulating device fabrication processes.

Photoluminescence Spectra. Photoluminescence (PL) spectroscopy is uniquely suitable to study molecular organization of highly conjugated polymers like the P3HT because the spectrum is sensitive to the state of aggregation of the chromophores. Time-resolved, dynamic fluorescence analysis was used to study the kinetics of gelation after quenching the system from the sol state to certain temperatures. In our experiments, a 1 mm sample cell in a front-face 30°/60° angle geometry was used for the measurement to minimize the self-filtering effects due to high optical densities or to sample turbidity. The PL spectra were found to be insensitive to the excitation wavelength in the range 330−500 nm. All emission spectra were obtained by excitation at the wavelength of the respective absorption maximum around 450 nm. The PL spectra of P3HT (Figures 5 and 6) show resolved vibronic structures at 570, 640, and 670

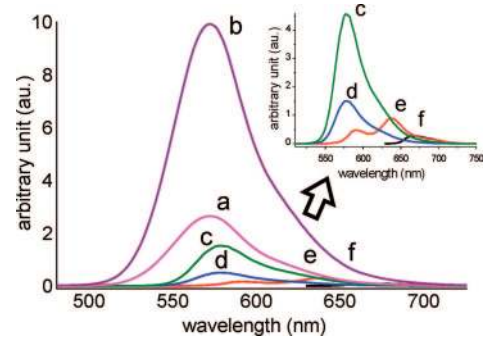

Figure 5. PL spectra of P3HT in *o*-xylene standing at room temperature for 30 min as a function of concentration: (a) 0.0002 wt %, (b) 0.002 wt %, (c) 0.02 wt %, (d) 0.5 wt %, (e) 1.0 wt %, and (f) 3.0 wt %.

nm. Yet before we employed PL to study molecular aggregation in gel-forming solutions, the PL spectra of freshly prepared *o*-xylene solutions of P3HT were acquired at room temperature (ca. 25 °C) over a wide range of concentrations, from 2×10^{-4} to 3 wt % (Figure 5). At low concentrations (curves a and b), the emission intensity increased almost proportionally with concentration. In this concentration regime, the molecules act as individuals or isolated chains[19,20] independent from each other, and the emission intensity at 570 nm is the sum of the individual concentrations. At higher concentrations (curves c, d, e, and f), the emission intensity decreased as concentration increased. Once the solution concentration reaches 0.02 wt % and beyond, self-quenching and other factors increase the probability for energy losses and cause a decrease in fluorescence efficiency and emission intensity. Significantly, two more emission bands at 640 and 670 nm were observed as the solution concentration increased to 1.0 wt % and beyond. This indicates that, although the emission maxima are located at the same wavelengths in all freshly prepared P3HT solutions regardless of concentration, the PL spectra must change in the course of gelation because the state of molecular aggregation cannot remain the same. In using PL to probe microstructure development that leads to gelation, the kinetics of emission of the 1.0 wt % P3HT *o*-xylene solution was monitored at 5, 25, and 70 °C, respectively, and the results are presented in Figure 6. This particular concentration was chosen because the aged gel was used for making devices and the time of gelation was appropriate for studies. At low temperatures (<5 °C), the emission spectra with a peak at 670 nm remained the same throughout the measurement, and eventually an opaque gel was formed. At 25 °C, a new peak at 640 nm appeared, and the peak intensity increased gradually with time. Concomitantly, the intensity of the 570 nm peak decreased with time but then underwent no further change after 1 h. Therefore, two different fluorescent species coexist before 1 h. At 70 °C, the fluorescence emission spectra did not change initially. With time, the fluorescence intensity at 570 nm decreased and the peak shifted to longer wavelength, and eventually a peak at ca. 640 nm was formed. The identities of the three species can be deduced from the following observations. First, the peak at 570 nm presents in the freshly prepared solution and also the same as the peak position in dilute solutions (Figure 5a). Second, the location of the featureless, broad peak at 640 nm is the same as that of solid-state emission due to aggregates/excimers (Figure 7a). Third, at low temperatures, the emission peak at 670 nm remains the same throughout the aging experiment, whicn is the same as that of solid-state emission from well-organized structures (Figure 7b) such as liquid crystalline samples. We therefore conclude that isolated chains, aggregates/excimers, and long-range order structures are presented in the 1.0 wt % P3HT solution at different conditions.

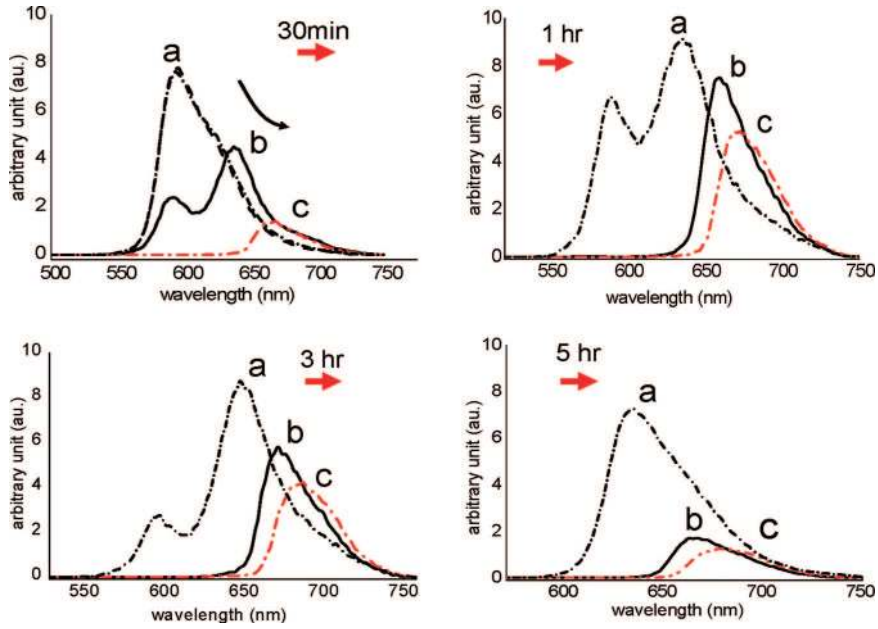

Figure 6. PL spectra of 1.0 wt % P3HT in *o*-xylene as a function of time and temperature: (a) 70 °C, (b) 25 °C, and (c) 5 °C.

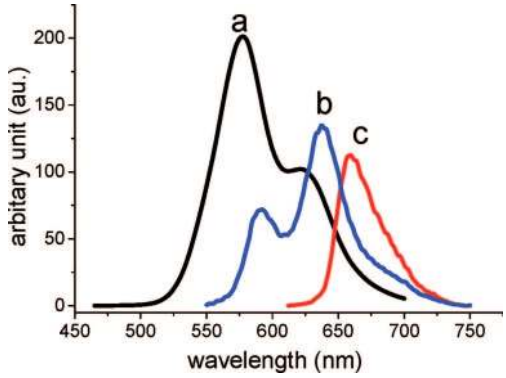

Figure 7. PL spectra of the P3HT thin films cast from (a) 1.0 wt % freshly prepared solution, (b) 1.0 wt % aged solution, and (c) 1.0 wt % aged solution and then annealed at 150 °C for 10 min.

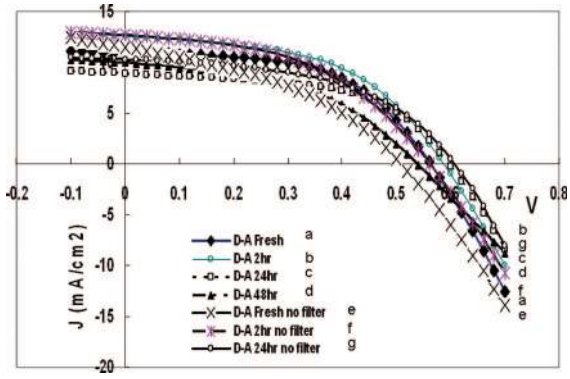

Figure 8. The *I*−*V* curves of P3HT/PCBM bulk heterojunction solar cells with the different photoactive layers spin-coated from variously aged solutions: (a) 0 h, (b) 2 h, (c) 24 h, and (d) 48 h with and (e) 0 h, (f) 2 h, and (g) 24 h without filtration.

Device Characterization. The *I*−*V* curves of P3HT/PCBM bulk heterojunction solar cells with the different photoactive layers spin-coated from variously aged solutions with and without filtration are shown in Figure 8, and the detailed photovoltaic properties are summarized in Table 2. Table 2 shows that all seven devices have similar values of open-circuit voltage (V_{oc}). This is due to the similar composition of photoactive layers for all devices. Interestingly, we also found that for those devices with photoactive layers spin-coated from the solutions with shorter aging time (devices a, b, e, and f), the short-circuit current density (J_{sc}) gradually increased; contrarily, it decreased considerably when the solutions are aged for a longer time (devices c, d, and g). This could be attributed to the morphological transitions in polymer solution and in the photoactive layer. The particle size of 1 wt % solution in *o*-xylene was measured by static light-scattering, and the results are tabulated in Table 3. It indicates that at an early stage of aging (<2 h) the structural redevelopment is initiated as the solution is quenched to room temperature and the mean diameter of P3HT molecules is less than 20 nm. However, molecular aggregation was observed after 3 h (mean diameter: 268 nm), and the mean diameter of aggregates gradually increased to 610 nm at 20 h, which could be attributed to microphase separation. As time passed (>24 h), a thermodynamically stable supramolecular organization could be attained, and thus concomitantly macrophase separation was reached in the solution, which matches previous results observed by UV−vis absorption, PL emission, and visualization studies. These changes influence several key processes in the photovoltaic cell, such as the photon absorption efficiency within the solar radiation spectrum, the charge separation efficiency at the donor−acceptor interface, the charge transport process toward the electrodes, and the

Table 2. Photovoltaic Properties of P3HT/PCBM Bulk Heterojunction Solar Cells with the Different Photoactive Layers

filtration	aged time	device	J_{sc} (mA/cm^2)	V_{oc} (volt)	FF	PCE (%)
with	0 h (fresh)	a	10.96	0.56	0.55	3.38
	2 h	b	12.57	0.59	0.51	3.78
	24 h	c	8.93	0.60	0.55	2.95
	48 h	d	9.94	0.54	0.46	2.47
without	0 h (fresh)	e	11.48	0.51	0.40	2.34
	2 h	f	12.65	0.56	0.47	3.33
	24 h	g	10.28	0.61	0.50	3.14

Table 3. Particle Size Measurement[a] of P3HT in *o*-Xylene at Room Temperature

aged time	<2 h	3 h	20 h	>24 h
mean diameter (nm)	NA [b] (<20)	268	610	NA[b] (>1000)

[a] The detection limits of measurement are located between 20 and 1000 nm. [b] Not applicable due to being out of the measurable range.

charge-transfer step at the electrodes. The overall effect of aging time leads to a strong influence in the short-circuit current and fill factor.

Device b (Table 2) demonstrates the current−voltage characteristics of the most effective P3HT/PCBM device, which shows the short-circuit current density of 12.57 mA/cm^2, the open-circuit photovoltage of 0.59 V, and the fill factor of 0.51. On the basis of these data, the PCE of the P3HT/PCBM device is evaluated as 3.78%, which is reasonably high, as compared to those previously reported using P3HT/PCBM composites.[9,10]

Conclusions

In summary, several different time-periods of solution aging can alter the efficiency and spectrum of OPV devices based on polymers. Among these, 2 h was the most proper aging time for improving the PV characteristics, as it showed the morphology of P3HT/PCBM composite in the scale of nanophase aggregation. Nanophase aggregation can increase the maximum electrical output due to the increased efficiency of charge separation, charge transport, and/or photon absorption. However, the quantum efficiency is lowered as aging time lengthens (>3 h) so that the aging time for device fabrication should be carefully controlled. A proper aging time reduces the scale of phase separation and greatly enhances the PV efficiency, and thus is recommended for a highly efficient PV device. These kinds of gelation effects can also be applied to other polymeric systems.

Acknowledgment. We wish to thank the National Science Council of Taiwan, under Grant Nos. NSC 97-2221-E-110-008 and NSC 96-2622-E-110-004, for supporting this research.

Supporting Information Available: Tapping mode AFM image of the film coated from the 1 h aged 1.0 wt % solution. This material is available free of charge via the Internet at http://pubs.acs.org.

References and Notes

(1) (a) Shaheen, S. E.; Brabec, C. J.; Sariciftci, N. S.; Padinger, F.; Fromherz, T.; Hummelen, J. C. *Appl. Phys. Lett.* **2001**, *78*, 841. (b) Chu, C. W.; Yang, H.; Hou, W. J.; Huang, J.; Li, G.; Yang, Y. *Appl. Phys. Lett.* **2008**, *92*, 103306.
(2) For recent reviews on PV cells, see: (a) Brabec, C. J.; Sariciftci, N. S.; Hummelen, J. C. *Adv. Funct. Mater.* **2001**, *11*, 15–26. (b) Coakley, K. M.; McGehee, M. D. *Chem. Mater.* **2004**, *16*, 4533–4542. (c) Gü nes, S.; Neugebauer, H. *Chem. Rev.* **2007**, *107*, 1324–1338.
(3) Janssen, R. A. J.; Hummelen, J. C.; Sariciftci, N. S. *MRS Bull.* **2005**, *30*, 28.
(4) Ma, W.; Yang, C.; Gong, X.; Lee, K.; Heeger, A. J. *Adv. Funct. Mater.* **2005**, *15*, 1617.
(5) Yang, X.; Loos, J. *Macromolecules* **2007**, *40*, 1353.
(6) Jin, S. H.; Naidu, B. V. K.; Jeon, H. S.; Park, S. M.; Park, J. S.; Kim, S. C.; Lee, J. W.; Gal, Y. S. *Sol. Energy Mater. Sol. Cells* **2007**, *91*, 1187.
(7) Yu, G.; Gao, J.; Hummelen, J. C.; Wudl, F.; Heeger, A. J. *Science* **1995**, *270*, 1789.
(8) Halls, J. J. M.; Walsh, C. A.; Greenham, N. C.; Marseglia, E. A.; Friend, R. H.; Moratti, S. C.; Holmes, A. B. *Nature* **1995**, *376*, 498.
(9) (a) Li, G.; Shrotriya, V.; Huang, J.; Yao, Y.; Yang, Y. *Nat. Mater.* **2005**, *4*, 864. (b) Padinger, F.; Rittberger, R. S.; Sariciftci, N. S. *Adv. Funct. Mater.* **2003**, *13*, 85.
(10) Kim, J. Y.; Kim, S. H.; Lee, H. H.; Lee, K.; Ma, W.; Gong, X.; Heeger, A. J. *Adv. Mater.* **2006**, *18*, 572.
(11) (a) Berson, S.; Bettignies, R. D.; Bailly, S.; Guillerez, S. *Adv. Funct. Mater.* **2007**, *17*, 1377. (b) Xin, H.; Kim, F. S.; Jenekhe, S. A. *J. Am. Chem. Soc.* **2008**, *130*, 5424. (c) Prosa, T. J.; Winokur, M. J.; Moulton, J.; Smith, P.; Heeger, A. J. *Macromolecules* **1992**, *25*, 4364.
(12) Schilinsky, P.; Asawapirom, U.; Scherf, U.; Biele, M.; Brabec, C. J. *Chem. Mater.* **2005**, *17*, 2175.
(13) Kim, Y.; Cook, S.; Tuladhar, S. M.; Choulis, S. A.; Nelson, J.; Durrant, J. R.; Bradley, D. D. C.; Giles, M.; McCulloch, I.; Ha, C. S.; Ree, M. *Nat. Mater.* **2006**, *5*, 197.
(14) Yue, S.; Berry, G. C.; McCullough, R. D. *Macromolecules* **1996**, *29*, 933.
(15) Shibaev, P. V.; Schaumburg, K.; Bjornholm, T.; Norgaard, K. *Synth. Met.* **1998**, *97*, 97.
(16) Li, L.; Collard, D. M. *Macromolecules* **2006**, *39*, 6092.
(17) Yamamoto, T.; Komarudin, D.; Arai, M.; Lee, B. L.; Suganuma, H.; Asakawa, N.; Inoue, Y.; Kubota, K.; Sasaki, S.; Fukuda, T.; Matsuda, H. *J. Am. Chem. Soc.* **1998**, *120*, 2047.
(18) Loewe, R. S.; Ewbank, P. C.; Liu, J.; Zhai, L.; McCullough, R. D. *Macromolecules* **2001**, *34*, 4324.
(19) Huang, W. Y.; Yung, H.; Lin, H. S.; Kwei, T. K.; Okamoto, Y. *Macromolecules* **1999**, *32*, 8089.
(20) Huang, W. Y.; Ho, S. W.; Kwei, T. K.; Okamoto, Y. *Appl. Phys. Lett.* **2002**, *80*, 1162.

MA801368Z